

DOPPLER-FREE SATURATED ABSORPTION SPECTROSCOPY: LASER SPECTROSCOPY

Overview

In this experiment you will use a diode laser to carry out laser spectroscopy of rubidium atoms. You will study the Doppler broadened optical absorption lines, and will then use the technique of saturated absorption spectroscopy to study the lines with resolution beyond the Doppler limit. This will enable you to measure the hyperfine splittings of one of the excited states of rubidium. You will use a Michelson interferometer to calibrate the frequency scale for this measurement. This experiment was developed by Carl Wieman and uses techniques currently in use in his and other research laboratories at CU. It is being duplicated at a number of other schools. To facilitate the widespread use of this experiment, which is new to undergraduate labs, Daryl Preston (author of your optional text), in collaboration with Wieman wrote a very lengthy writeup. The purpose of this writeup was to allow schools to duplicate the experiment, even if the lab instructors were not familiar with laser spectroscopy. As a result, it is somewhat different in style and far more detailed than your other writeups have been. Although it is long, it does explain in detail everything you will need to know to carry out and analyze this experiment so you will have little need of other references. References to other chapters or experiments refer to items in Preston's book "The Art of Experimental Physics".

Historical Note

One half of the 1981 Nobel prize in Physics was awarded jointly to Arthur L. Schawlow, Stanford University. During the 70's, Professor Schawlow's research group developed and applied the technique of Doppler-Free Saturation Absorption Spectroscopy.

Apparatus

Tunable 780-nm diode laser system (see reference 1)
Rubidium vapor cell
Photodiode detector circuit (see reference 1)
Triangle waveform generator
2' x 2' x 1/2" optical breadboard
3/8"-thick transparent plastic or glass (beam splitter)
4 flat mirrors
4 mirror mounts
9 posts (for mounting vapor cell, photodiode detectors, mirrors, and beam splitter)
Oscilloscope (Optional: storage scope with a plotter)
Oscilloscope camera
Kodak IR detection card
Hand held IR viewer or a CCD surveillance camera

Purpose

- 1) To appreciate the distinction between linear and nonlinear spectroscopy.
- 2) To understand term states, fine structure, and hyperfine structure of rubidium.
- 3) To record and analyze the Doppler-broadened 780-nm rubidium spectral line (linear optics).
- 4) To record and analyze the Doppler-free saturated absorption lines of rubidium (nonlinear optics), and thereby determine the hyperfine splitting of the $5P_{3/2}$ state.

Key Concepts

Linear optics	Electric dipole selection rules
Nonlinear optics	Doppler broadening
Absorption spectroscopy	Fine structure
Saturated absorption spectroscopy	Hyperfine structure

References

1. K. B. MacAdam, A. Steinbach, and C. Wieman, *Am. J. Phys.* 60, 1098-1111, 1992. The construction of the diode laser system and the Doppler-free saturated absorption experiment are discussed in detail in this paper. Parts, suppliers, and cost are listed.
2. M. D. Levenson, Introduction to Nonlinear Laser Spectroscopy, Academic Press, 1982
3. Carl E. Wieman and Leo Hollberg, *Rev. Sci. Instrum.* 62(1), January 1991, pp. 1-20. Diode lasers in atomic physics are reviewed. The list of references is extensive.
4. J. C. Camparo, *Contemp. Phys.*, Vol. 26, No. 5, 1985, 443-477. This is the first paper to review the diode laser in atomic physics.
5. A. Corney, Atomic and Laser Spectroscopy. Oxford Press 1977. Hyperfine interactions are discussed in chapter 18.
6. V. S. Letokhov, "Saturation Spectroscopy", Chapter 4 of High Resolution Laser Spectroscopy (Topics in Applied Physics, Vol. 13, ed. K. Shimoda), Springer-Verlag, 1976.
7. T. W. Hansch, Nonlinear high resolution spectroscopy of atoms and molecules, in "Nonlinear Spectroscopy" (Proc. Int. School Phys., Enrico Fermi, Course 64) (N. Bloembergen, ed.). North-Holland Publi. Amsterdam, 1977.
8. W. Demtroder, Laser Spectroscopy (Springer series in Chemical Physics, Vol. 5), Springer, New York, 1982.
9. E. Arimondo, M. Inguscio, and P. Violino, *Rev. Mod. Phys.*, Vol. 49, No. 1, 1977. The experimental determinations of the hyperfine structure in the alkali atoms are reviewed.
10. R. Gupta, *Am. J. Phys.* 59(10), 874 (1991). This paper is a Resource Letter that provides a guide to literature on laser spectroscopy.
11. T. W. Hansch, A. L. Schawlow, and G. W. Series, *Sci. Am.* 240(18), 94 (March 1979). An excellent semi-quantitative discussion of laser spectroscopy with many good figures.

Introduction

Figure 1 compares an older method with a modern method of doing optical spectroscopy. Figure 1a shows the energy levels of atomic deuterium and the allowed transitions for $n = 2$ and 3, 1b shows the Balmer α emission line of deuterium recorded at 50 K with a spectrograph, where the vertical lines in 1b are the theoretical intensities, and 1c shows an early high resolution laser measurement, where one spectral line is arbitrarily assigned 0 cm^{-1} . The "crossover" resonance line shown in 1c will be discussed later. (See figure 12.3 for more details on the energy levels of hydrogen.) Even at 50 K the emission lines are Doppler-broadened by the random thermal motion of the emitting atoms, while the laser method using a technique known as Doppler-free, saturated absorption spectroscopy eliminates Doppler-broadening.

What feature of the laser gives rise to high resolution spectroscopy? Well, it is the narrow spectral linewidth, which is about 20 MHz for the diode laser, and the tunability of lasers that have revolutionized optical spectroscopy. Note that when the 780-nm diode laser is operating at its center frequency then most of its power output is in the frequency range of $3.85 \times$

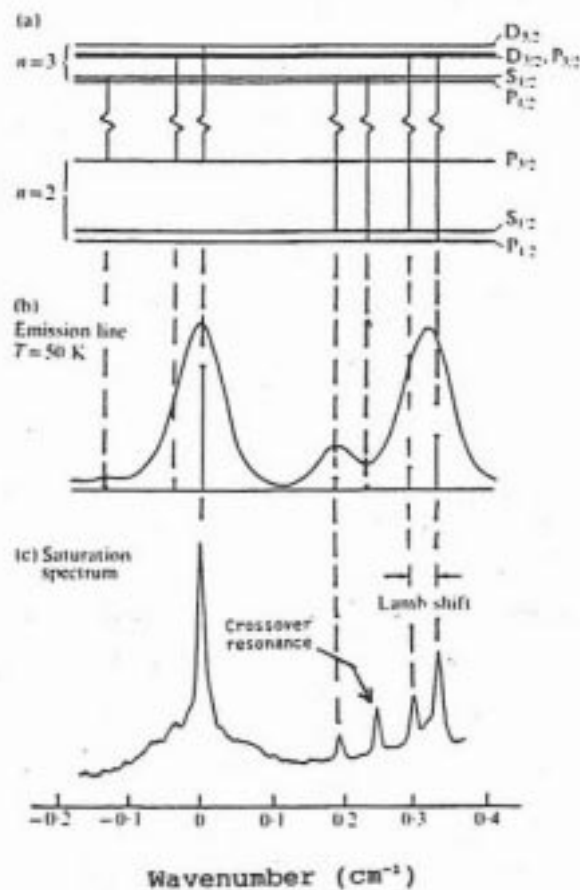


Figure 1. The Balmer α line of atomic deuterium: (a) Energy levels and allowed transitions, (b) the emission spectrum, (c) an early saturated absorption spectrum.

10^{14} Hz \pm 10×10^6 Hz. Reference 1 points out a method of reducing the spectral linewidth to less than 1 MHz.

The topics to be discussed in the Introduction are linear and nonlinear optics, diode laser, atomic structure of rubidium, absorption spectroscopy and Doppler broadening, and Doppler-free saturated absorption spectroscopy.

A simplified diagram of linear spectroscopy is shown in figure 2a, where a single propagating wave is incident on the sample, some photons are absorbed, as shown in the two-level energy diagram, and some fraction of the wave reaches the detector. Nonlinear spectroscopy is illustrated in figure 2b, where there are two counterpropagating waves that interact with the same atoms in the region where they intersect. The beam propagating to the right, the “pump” beam, causes the transition indicated with a dashed line in the energy level diagram, and the beam propagating to the left, the “probe” beam, causes the transition indicated with a solid line. In this case the field reaching the detector is a function of both fields, hence, nonlinear spectroscopy.

Prior to the development of the laser, the interaction between optical frequency fields and matter were weak enough that linear theories were adequate.

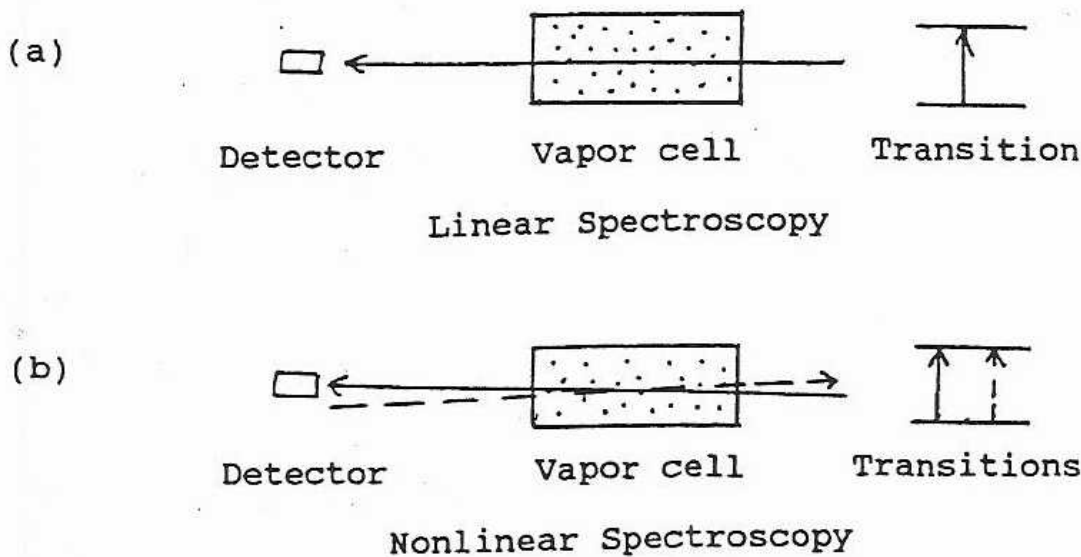


Figure 2. In linear spectroscopy (a) the radiation reaching the detector is proportional to the radiation incident on the sample, and in nonlinear spectroscopy (b) the radiation reaching the detector is dependent on both beams.

Diode Laser

The discussion and figures in this section are for the Sharp 780-nm, LT025MD0 diode laser. Figure 3 shows the diode laser with a cut-away of the housing where the chip mounts. Figure 4 shows the laser chip structure, typical chip dimensions, the direction of the forward current, and the radiation pattern. The radiation is produced in the active layer, which is a small fraction of the height of the chip, hence the radiation is diffracted when it emerges from the active region analogously to the diffraction of radiation passing through a narrow slit. The diffraction produces the radiation pattern shown in figure 4. Figure 5 shows the optical power

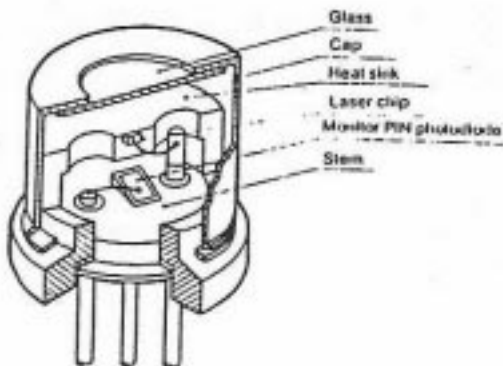


Figure 3. Internal structure of the Sharp LT025MD0 diode laser.

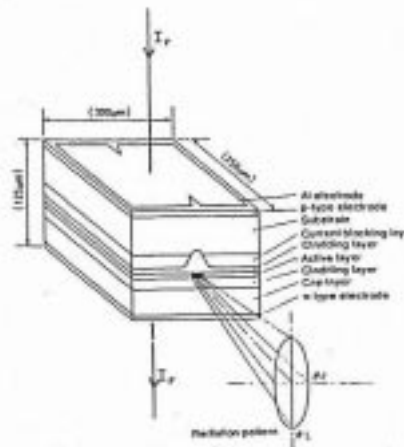


Figure 4. Chip structure of the Sharp LT025MD0 diode laser.

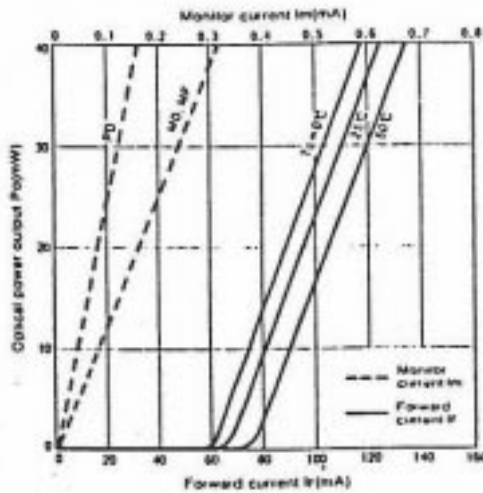


Figure 5. Optical power output versus forward current (for three laser temperatures) and monitor current.

Exercise 1.

The index of refraction of GaAs and air are about 3.6 and 1.0. What is the reflectivity of the chip facet? Compare your answer with the reflectivity of the mirrors used in the HeNe laser, which is about 0.99.

Exercise 2

Assuming the length of the diode laser cavity is 250 μm and the index of refraction of the cavity is 3.6, show that the frequency spacing $\Delta\nu$ of the axial modes is 167 GHz. (You may want to refer to the discussion of axial modes under Laser Cavity Modes of the Introduction to Laser Physics.)

The LT025MD0 diode laser has a reduced reflective coating on the output facet of the chip; therefore, the reflectivity of this facet is less than that calculated in Exercise 1. The grating reflectivity is about 40%, hence it dominates the front facet of the chip in forming the laser cavity. Therefore, the length of the cavity is the distance from the grating to the far chip facet. The purpose of this configuration is to change the laser wavelength by displacing the grating.

output versus forward current and monitor current. The maximum operating forward current and power output are specified by the manufacturer for each diode laser. Figure 6 shows the wavelength versus case temperature. Figure 7 shows how the power output depends on the wavelength, where the spectral width of the laser line at 30 mW is about 20 MHz.

The mirrors for a diode laser chip are the cleaved facets of the semiconductor, which are smoother and flatter than any mechanically polished mirror. If there are no coatings on the end surfaces of the laser chip, then the reflectivity R of a surface is given by

$$R = \left(\frac{n_c - n_a}{n_c + n_a} \right)^2 \quad (3)$$

where n_c and n_a are the indices of refraction of the chip and air, respectively.

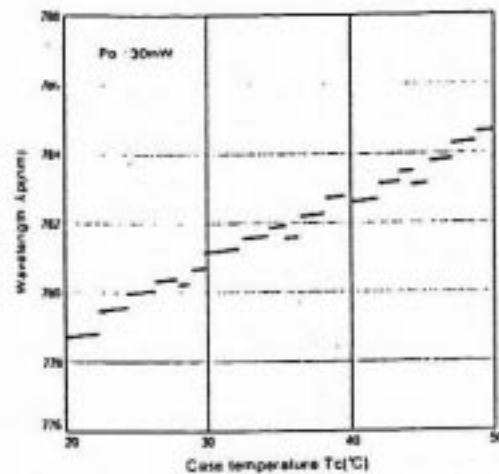


Figure 6. Emitted wavelength versus case temperature. Note the discontinuities.

Atomic Structure of Rubidium

The ground electron configuration of Rb is: $1s^2; 2s^2, 2p^6; 3s^2, 3p^6, 3d^{10}; 4s^2, 4p^6; 5s^1$, and with its single $5s^1$ electron outside of closed shells it has an energy-level structure that resembles hydrogen. For Rb in its first excited state the single electron becomes a $5p^1$ electron. Also natural rubidium has two isotopes, the 28% abundant ^{87}Rb , where the nuclear spin quantum number $I = 3/2$, and the 72% abundant ^{85}Rb , where $I = 5/2$.

Term States

A term state is a state specified by the angular momenta quantum numbers s , l , and j (or S , L , and J), and the notation for such a state is $^{2s+1}l_j$ (or $^{2s+1}L_j$). The spectroscopic notation for l values is $l = 0(\text{S}), 1(\text{P}), 2(\text{D}), 3(\text{F}), 4(\text{G}), 5(\text{H}), \dots$

The total angular momentum \mathbf{J} is defined by

$$\mathbf{J} = \mathbf{L} + \mathbf{S} \quad (J_s) \quad (4)$$

where their magnitudes are

$$J = \hbar\sqrt{j(j+1)}; L = \hbar\sqrt{l(l+1)}; S = \hbar\sqrt{s(s+1)} \quad (5)$$

and the possible values of the total angular momentum quantum number j are $|l - s|, |l - s| + 1, \dots, l + s - 1, l + s$; where for a single electron $s = 1/2$. It is recommended that you read the discussion on LS coupling and term

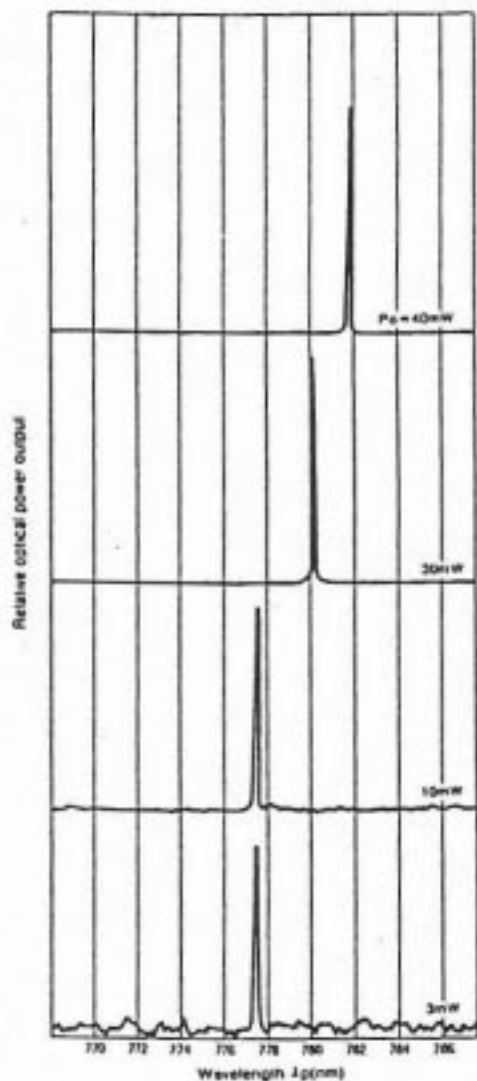


Figure 7. Power output dependence of wavelength.

states in Experiment 16.

The $5s^1$ electron gives rise to a $5^2S_{1/2}$ ground term state. The first excited term state corresponds to the single electron becoming a $5p^1$ electron, and there are two term states, the $5^2P_{1/2}$ and the $5^2P_{3/2}$.

Exercise 3

Show for a $5s^1$ electron that the term state is a $5^2S_{1/2}$. For a $5p^1$ electron show that the term states are $5^2P_{1/2}$ and $5^2P_{3/2}$.

Hamiltonian

Assuming an infinitely massive nucleus, the nonrelativistic Hamiltonian for an atom having a single electron is given by

$$H = \frac{p^2}{2m} - \frac{Z_{\text{eff}} e^2}{4\pi\epsilon_0 r} + \zeta(r) \mathbf{L} \cdot \mathbf{S} + \alpha \mathbf{J} \cdot \mathbf{I} + \frac{\beta}{2I(2I-1)J(2J-1)} \left[3(\mathbf{I} \cdot \mathbf{J})^2 + \frac{3}{2}(\mathbf{I} \cdot \mathbf{J}) - I(I+1)J(J+1) \right] (J) \quad (6)$$

We label the 5 terms in this equation, in order, as K , V , H_{so} , $H_{1,\text{hyp}}$, and $H_{2,\text{hyp}}$ respectively. K is the kinetic energy of the single electron; where $p = i\hbar\nabla$. Classically \mathbf{p} is the mechanical momentum of the electron of mass m . V is the Coulomb interaction of the single electron with the nucleus and the core electrons (this assumes the nucleus and core electrons form a spherical symmetric potential with charge $Z_{\text{eff}}e$, where Z_{eff} is an effective atomic number).

H_{so} is the spin orbit interaction, where \mathbf{L} and \mathbf{S} are the orbital and spin angular momenta of the single electron. $H_{1,\text{hyp}}$ is the magnetic hyperfine interaction, where \mathbf{J} and \mathbf{I} are the total electron and nuclear angular momenta, respectively. This interaction is $-\boldsymbol{\mu}_n \cdot \mathbf{B}_e$ where $\boldsymbol{\mu}_n$, the nuclear magnetic dipole moment, is proportional to \mathbf{I} , and \mathbf{B}_e , the magnetic field produced at the nucleus by the single electron, is proportional to \mathbf{J} . Hence the interaction is expressed as $\alpha \mathbf{I} \cdot \mathbf{J}$. α is called the magnetic hyperfine structure constant, and it has units of energy, that is, the angular momenta \mathbf{I} and \mathbf{J} are dimensionless. $H_{2,\text{hyp}}$ is the electric quadrupole hyperfine interaction, where β is the electric quadrupole interaction constant, and nonbold I and J are angular momenta quantum numbers. The major electric pole of the Rb nucleus is the spherical symmetric electric monopole, which gives rise to the Coulomb interaction; however, it also has an electric quadrupole moment (but not an electric dipole moment). The electrostatic interaction of the single electron with the nuclear electric quadrupole moment is $-eV_q$, that is, it is the product of the electron's charge and the electrostatic quadrupole potential. Although it is not at all obvious, this interaction can be expressed in terms of \mathbf{I} and \mathbf{J} . In both hyperfine interactions \mathbf{I} and \mathbf{J} are dimensionless, that is, the constants α and β have units of joules.

We will not use the above Hamiltonian in the time independent Schrodinger equation and solve for the eigenvalues or quantum states of Rb, but rather we present a qualitative discussion of how each interaction effects such states.

$K + V$

The $K + V$ interactions separate the 5s ground configuration and the 5p excited configuration. This is shown in figure 8a. Qualitatively, if the potential energy is not a strictly Coulomb potential energy then for a given value of n , electrons with higher l have a higher orbital angular momentum (a more positive kinetic energy) and on the average are farther from the nucleus (a less negative Coulomb potential energy), hence higher l value means a higher (more positive) energy. This scenario does not occur in hydrogen because the potential energy is coulombic.

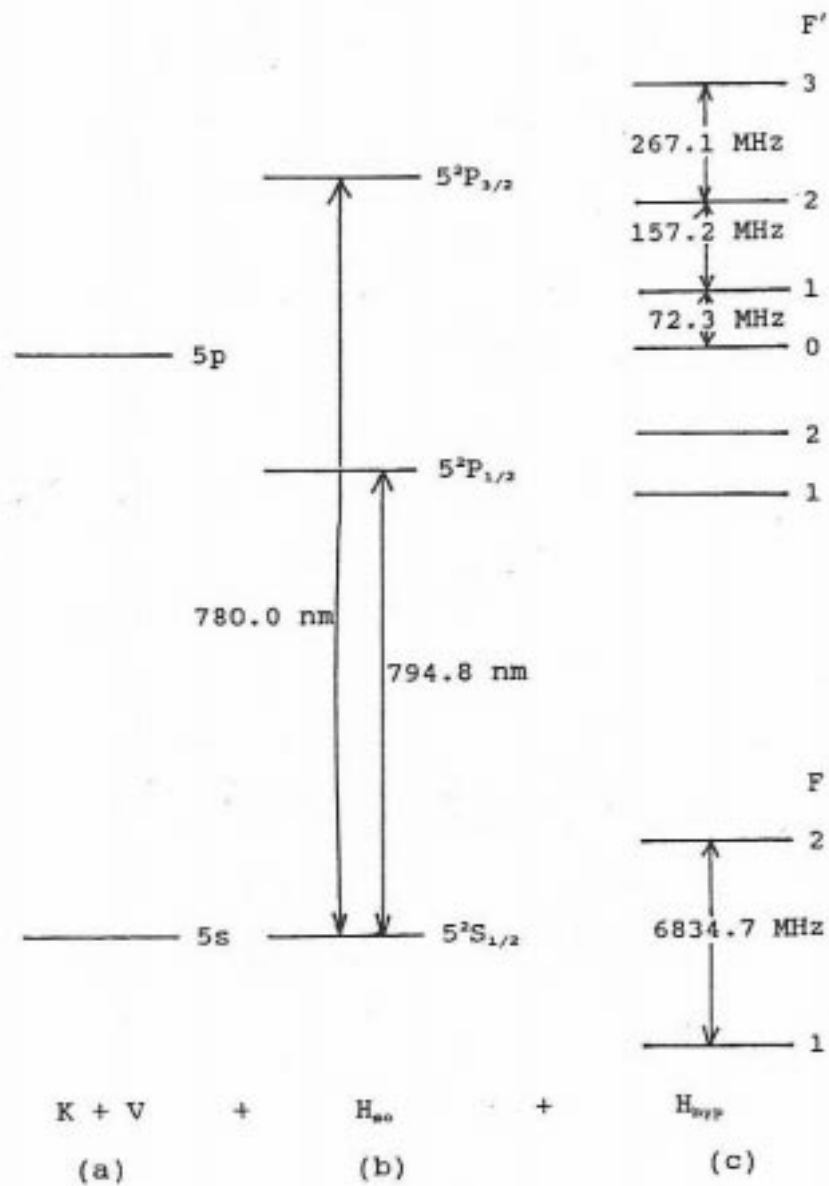


Figure 8. Each interaction in equation 6 and its effect on the energy levels of the 5s and 5p electron is shown. The energy level spacings are not to scale. The hyperfine levels are for ^{87}Rb .

Fine Structure; H_{so}

The spin-orbit interaction and its physical basis are discussed in Experiment 16. Fine structure is discussed in Experiment 12, where it is pointed out that fine structure, the splitting of spectral lines into several distinct components, is found in all atoms. The interactions that give rise to fine structure does depend on the particular atom. Ignoring relativistic terms in H , it is H_{so} that produces the fine structure splitting of Rb.

Using equation (4) and forming the dot product of $\mathbf{J}\cdot\mathbf{J}$, we solve for $\mathbf{L}\cdot\mathbf{S}$ and obtain

$$\begin{aligned}
L \cdot S &= (J^2 - L^2 - S^2) / 2 \\
&= (\hbar^2 / 2)[j(j+1) - \ell(\ell+1) - s(s+1)]
\end{aligned}
\tag{7}$$

where the magnitudes of the vectors were used in the last equality. Using equation (7), H_{so} can be written

$$H_{so} = \zeta(r)(\hbar^2 / 2)[j(j+1) - \ell(\ell+1) - s(s+1)] \tag{8}$$

Exercise 4

Show that the splitting of the $5^2P_{1/2}$ and the $5^2P_{3/2}$ term states due to H_{so} is $\zeta(r)3\hbar^2 / 2$.

Figure 8b shows the effect of H_{so} on the quantum states. The separation of the $5^2S_{1/2}$ and the $5^2P_{3/2}$ states, in units of wavelength, is 780.023 nm, and the separation of the $5^2S_{1/2}$ and the $5^2P_{1/2}$ states is 794.764 nm. It is the transition between the $5^2S_{1/2}$ and the $5^2P_{3/2}$ states that will be studied using the 780-nm laser.

Hyperfine Structure; H_{hyp}

For either hyperfine interaction, the interaction couples the electron angular momentum \mathbf{J} and the nuclear angular momentum \mathbf{I} to form the total angular momentum, which we label as \mathbf{F} , where

$$\mathbf{F} = \mathbf{J} + \mathbf{I} \quad (\mathbf{J}) \quad (9)$$

and the possible quantum numbers F are $|J - I|, |J - I + 1|, \dots, J + I - 1, J + I$. (In this case the nonbold capital letters are being used for quantum numbers, which, for the hyperfine interaction, is more standard practice than using f, j and i as the quantum numbers.)

Exercise 5

For ^{87}Rb show: (1) for the $5^2S_{1/2}$ state that $F = 1, 2$; (2) for the $5^2P_{1/2}$ state that $F = 1, 2$; (3) for the $5^2P_{3/2}$ state that $F = 0, 1, 2, 3$.

The hyperfine structure of both ^{85}Rb and ^{87}Rb will be observed in this experiment; however, it is the hyperfine structure of ^{87}Rb that will be studied. The energy levels in figure 8b are split by the hyperfine interaction into the levels shown in 8c for ^{87}Rb . The levels in 8c are known as hyperfine levels, where the total angular momentum quantum numbers are labeled as F' and F for the $5^2P_{3/2}$ and the $5^2S_{1/2}$ states, respectively. The selection rules for electric dipole transitions are given by

$$\begin{aligned}
\Delta F &= 0 \text{ or } \pm 1 \text{ (but not } 0 \rightarrow 0) \\
\Delta F &= 0 \text{ or } \pm 1 \\
\Delta S &= 0
\end{aligned}
\tag{10}$$

Exercise 6

Assuming all of the spectral lines are resolved for transitions from the $5^2P_{3/2}$ excited state to the $5^2S_{1/2}$ ground state, how many spectral lines do you expect to observe for ^{87}Rb ?

In addition to the normal resonance lines, there are “crossover” resonances peculiar to saturated absorption spectroscopy, which occur at frequencies $(\nu_1 + \nu_2)/2$ for each pair of true or normal transitions at frequency ν_1 and ν_2 . A crossover resonance is indicated in figure 1c. The crossover transitions are often more intense than the normal transitions. In figure 9 six crossover transitions, b, d, e, h, j, and k, and six normal transitions, a, c, f, g, i, and l, are shown, where for the normal transitions $\bullet F = 0, \pm 1$. The frequency of the emitted radiation increases from a to l.

What are the expected frequencies of the normal transitions a, c, f, g, i, and l? To answer this question we first determine the energies of the hyperfine levels. Using equation 9 and forming the dot product of $\mathbf{F} \cdot \mathbf{F}$, we solve for $\mathbf{J} \cdot \mathbf{I}$ and obtain

$$\begin{aligned} \mathbf{J} \cdot \mathbf{I} &= (F^2 - J^2 - I^2) / 2 \\ &= [F(F+1) - J(J+1) - I(I+1)] / 2 \quad (11) \\ &= C / 2 \end{aligned}$$

where dimensionless magnitudes were used in the second equality and the last equality defines C. Replacing $\mathbf{J} \cdot \mathbf{I}$ in the hyperfine interactions of equation 6 with equation 11, the magnitude of the interactions or the energy $E_{J,F}$ is given by

$$\begin{aligned} E_{J,F} &= E_J + E_{hyp} \\ &= E_J + \alpha \frac{C}{2} + \beta \frac{\frac{3}{4}C^2 + \frac{3}{4}C - I(I+1)J(J+1)}{2I(2I-1)J(2J-1)} \quad (J) \quad (12) \end{aligned}$$

where E_J is the energy of the $n^{2S+1}L_J$ state, that is, the $5^2P_{3/2}$ or the $5^2S_{1/2}$ state shown in figure 9. From figure 9 note that in equation 12 for the $5^2P_{3/2}$ state $I = 3/2$, $J = 3/2$, and $F = 0, 1, 2, 3$; and for the $5^2S_{1/2}$ state $I = 3/2$, $J = 1/2$, and $F = 1, 2$.

(drawing) (fig 9)

The frequencies $\nu_{J,F}$ (energy/h) of the various hyperfine levels are obtained by dividing equation 12 by Planck's constant h:

$$\nu_{J,F} = \nu_J + A \frac{C}{2} + B \frac{\left[\frac{3}{4}C(C+1) - I(I+1)J(J+1) \right]}{2I(2I-1)J(2J-1)} \quad (\text{Hz}) \quad (13)$$

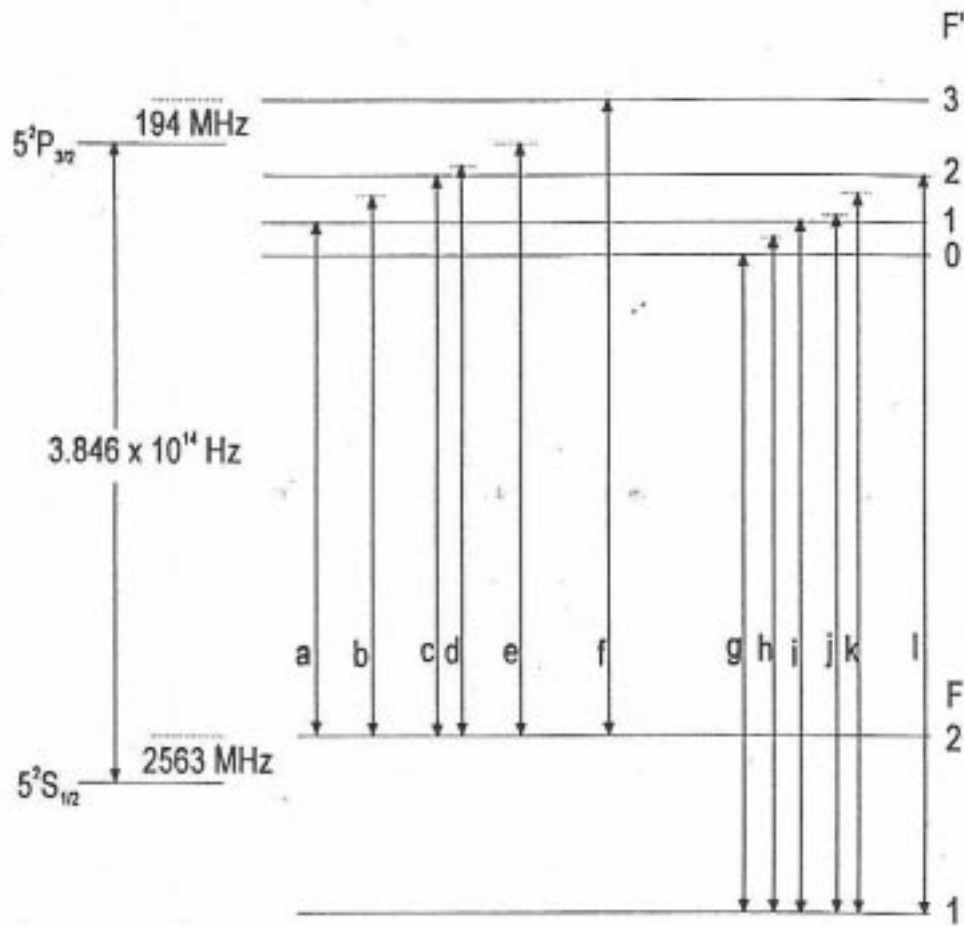


Figure 9. Saturated absorption transitions for ^{87}Rb . The spectral line separation will be derived in exercises 6 through 8 or can be figured out from figure 8.

where $A \equiv \alpha/h$ and $B \equiv \beta/h$ have units of hertz.

For the $5^2S_{1/2}$ state of ^{87}Rb , the term that multiplies B in equation 13 reduces to zero and the accepted value of A is 3417.34 MHz. For the $5^2P_{3/2}$ state of ^{87}Rb , the accepted values of A and B are 84.85 MHz and 12.52 MHz, respectively. For the $5^2S_{1/2}$ of ^{85}Rb the accepted value of A is 1011.91 MHz, and for the $5^2P_{3/2}$ the accepted values of A and B are 25.01 MHz and 25.9 MHz, respectively.

Exercise 7

For the $5^2S_{1/2}$ state of ^{87}Rb substitute numerical values for I , J , and F into the third term of equation 13 and show for both $F = 1$ and 2 that this formula only makes sense if $B = 0$ for these two cases

Exercise 8

For ^{87}Rb use equation 13 to show that: (1) for the $5^2S_{1/2}$ state the splitting of the $F = 1$ and $F = 2$ levels, $\nu_{1/2,2} - \nu_{1/2,1}$ is 6834.7 MHz, as shown in figure 8c, (2) for the $5^2P_{3/2}$ state the splitting

of the $F' = 3$ and $F' = 2$ levels, $\nu_{3/2,3} - \nu_{3/2,2}$ is 267.1 MHz, as shown in figure 8c, (3) the frequency spacing $\bullet\nu = \nu_{3/2,2} - \nu_{J=3/2}$ is 194.0 MHz as shown in figure 9. (4) Now that you know how to do the calculations using equation 13, just use the energy level spacings given in figures 8 and 9 to show the frequency of transitions a and b are $3.846 \times 10^{14} - 2.7933 \times 10^9$ Hz and $3.846 \times 10^{14} - 2.7147 \times 10^9$ Hz, respectively, hence the separation of these two spectral lines is 79 MHz. (5) Show that the frequency separation of spectral lines a and I is 6.993 GHz and then show that their wavelength separation is 0.0142 nm.

One goal of this experiment is to experimentally determine A and B for the $5^2P_{3/2}$ state of ^{87}Rb .

Doppler Broadening and Absorption Spectroscopy

Random thermal motion of atoms or molecules creates a Doppler shift in the emitted or absorbed radiation. The spectral lines of such atoms or molecules are said to be Doppler broadened since the frequency of the radiation emitted or absorbed depends on the atomic velocities. (The emission spectral lines in both Experiments 12 and 13 will be Dopplerbroadened.) Individual spectral lines may not be resolved due to Doppler broadening, and, hence, subtle details in the atomic or molecular structure are not revealed. What determines the linewidth of a Doppler broadened line? To answer this question we do some theoretical physics.

We first consider the Doppler effect qualitatively. If an atom is moving toward or away from a laser light source, then it “sees” radiation that is blue or red shifted, respectively. If an atom at rest, relative to the laser, absorbs radiation of frequency ν_0 , then when the atom is approaching the laser it will see blue-shifted radiation, hence for absorption to occur the frequency of the laser must be less than ν_0 in order for it to be blue-shifted to the resonance value of ν_0 . Similarly, if the atom is receding from the laser, the laser frequency must be greater than ν_0 for absorption to occur.

We now offer a more quantitative argument of the Doppler effect and atomic resonance, where, as before, ν_0 is the atomic resonance frequency when the atom is at rest in the frame of the laser. If the atom is moving along the z-axis, say, relative to the laser with $v_z \ll c$, then the frequency of the absorbed radiation in the rest frame of the laser will be ν_L , where

$$\nu_L = \nu_0 \left(1 + \frac{v_z}{c} \right). \quad (\text{Hz}) \quad (14)$$

If v_z is negative (motion toward the laser) then $\nu_L < \nu_0$, that is, the atom moving toward the laser observes radiation that is blue-shifted from ν_L up to ν_0 . If v_z is positive (motion away from the laser) then $\nu_L > \nu_0$, that is, the atom observes radiation that is red-shifted from ν_L down to ν_0 . Therefore, an ensemble of atoms having a distribution of speeds will absorb light over a range of frequencies.

The probability that an atom has a velocity between v_z and $v_z + dv_z$ is given by the Maxwell distribution

$$P(v_z) dv_z = \left(\frac{M}{2\pi kT} \right)^{1/2} \exp\left(-\frac{Mv_z^2}{2kT} \right) dv_z \quad (15)$$

where M is the mass of the atom, k is the Boltzmann constant, and T is the absolute temperature. From equation 14

$$v_z = (v_L - v_0)c/v_0; \quad dv_z = c dv_L/v_0 \quad (\text{m/s}) \quad (16)$$

Substituting (16) into (15), the probability of absorbing a wave with a frequency between v_L and $v_L + dv_L$ is given in terms of the so-called linewidth parameter $\delta \equiv 2(v_0/c)(2kT/M)^{1/2}$ by

$$P(v_L) dv_L = \frac{2}{\delta\sqrt{\pi}} \exp(-4(v_L - v_0)^2 / \delta^2) dv_L \quad (17)$$

The half width, which is the full-width at half maximum amplitude (FWHM), of the Dopplerbroadened line is given by

$$\Delta v_{1/2} = \delta(\ln 2)^{1/2} = 2 \frac{v_0}{c} \left(\frac{2kT}{M} \ln 2 \right)^{1/2} \quad (\text{Hz}) \quad (18)$$

The profile of a Doppler-broadened spectral line is shown in figure 10. Substituting numerical values for the constants, equation 18 becomes

$$\Delta v_{1/2} = 2.92 \times 10^{-20} v_0 \left(\frac{T}{M} \right)^{1/2} \quad (19)$$

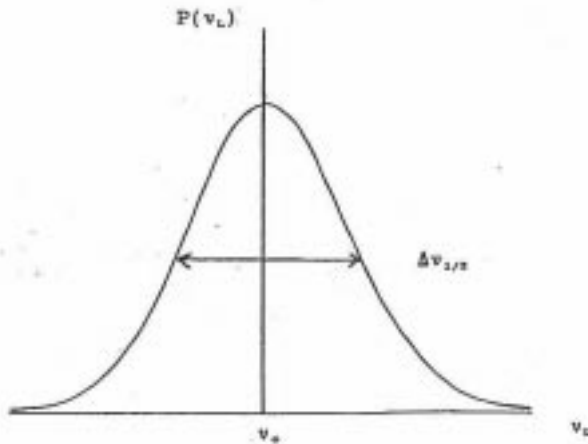


Figure 10. Doppler-broadened spectral line, where $\Delta v_{1/2}$ is the FWHM and v_0 is the absorbed frequency when the atom is at rest in the frame of the laser.

where M is the mass of the absorbing atom in kilograms and T is the absolute temperature in kelvins. So from equation 18 the FWHM of a Doppler broadened line is a function of v_0 , M , and T .

Exercise 9

Show that the FWHM of the 780-nm spectral line of Rb at 297 K due to Dopplerbroadening is 513 MHz.

The spectral absorption lines you will observe using absorption spectroscopy will be Doppler-broadened. However, the absorption lines you will observe using saturated absorption spectroscopy will not be Doppler-broadened, in fact, they will

approach the minimum or natural linewidth determined by the Heisenberg uncertainty principle.

Exercise 10

For an atom with no Doppler shift, the linewidth is determined by the Heisenberg uncertainty principle, $\Delta E \approx \hbar / \tau$, where τ is the excited state lifetime, and the range of frequencies absorbed is given by $\Delta \nu \approx 1 / 2\pi\tau$. From the expression for $\Delta \nu$ make a reasonable estimation of an expression for the FWHM, $\Delta \nu_{1/2}$, and using the 28-ns lifetime of the $^2P_{3/2}$ excited state of ^{87}Rb calculate the FWHM. Compare your answer to the 513 MHz FWHM in Exercise 9.

Exercise 11

When you perform absorption spectroscopy on ^{87}Rb how many spectral lines do you predict will be resolved? To answer this question use the 513 MHz FWHM from Exercise 9 and use the spectral line separations that are given in figure 9.

Doppler-Free Saturated Absorption Spectroscopy

The apparatus for the Doppler-free saturated absorption spectroscopy of Rb is shown in figure 11. The output beam from the laser is split into three beams, two less intense probe beams and a more intense pump beam, at the beamsplitter BS. The two probe beams pass through the Rb cell from left to right, and they are separately detected by two photodiodes. After being reflected twice by mirrors M1 and M2, the more intense pump beam passes through the Rb cell from right to left. Inside the Rb cell there is a region of space where the pump and a probe beam overlap and, hence, interact with the same atoms. This overlapping probe beam will be referred to as the first probe beam and the other one the second probe beam.

The signal from the second probe beam will be a linear, absorption spectroscopy signal, where the spectral lines will be Doppler-broadened. The signal is shown in figure 12a, and it was photographed from the screen of an oscilloscope. This signal was obtained by blocking the pump and first probe beams. There are two Doppler-broadened lines shown in the 12a, and a portion of the triangular waveform that drives the PZT, and hence, sweeps the laser frequency, is also shown. The larger amplitude signal is that of the 72% abundant ^{85}Rb and the smaller amplitude signal is that of the 28% abundant ^{87}Rb . The ^{87}Rb transition is the $F = 2$ to $F' = 1, 2$ and 3 transition, and the ^{85}Rb transition is $F = 3$ to $F' = 2, 3$, and 4.

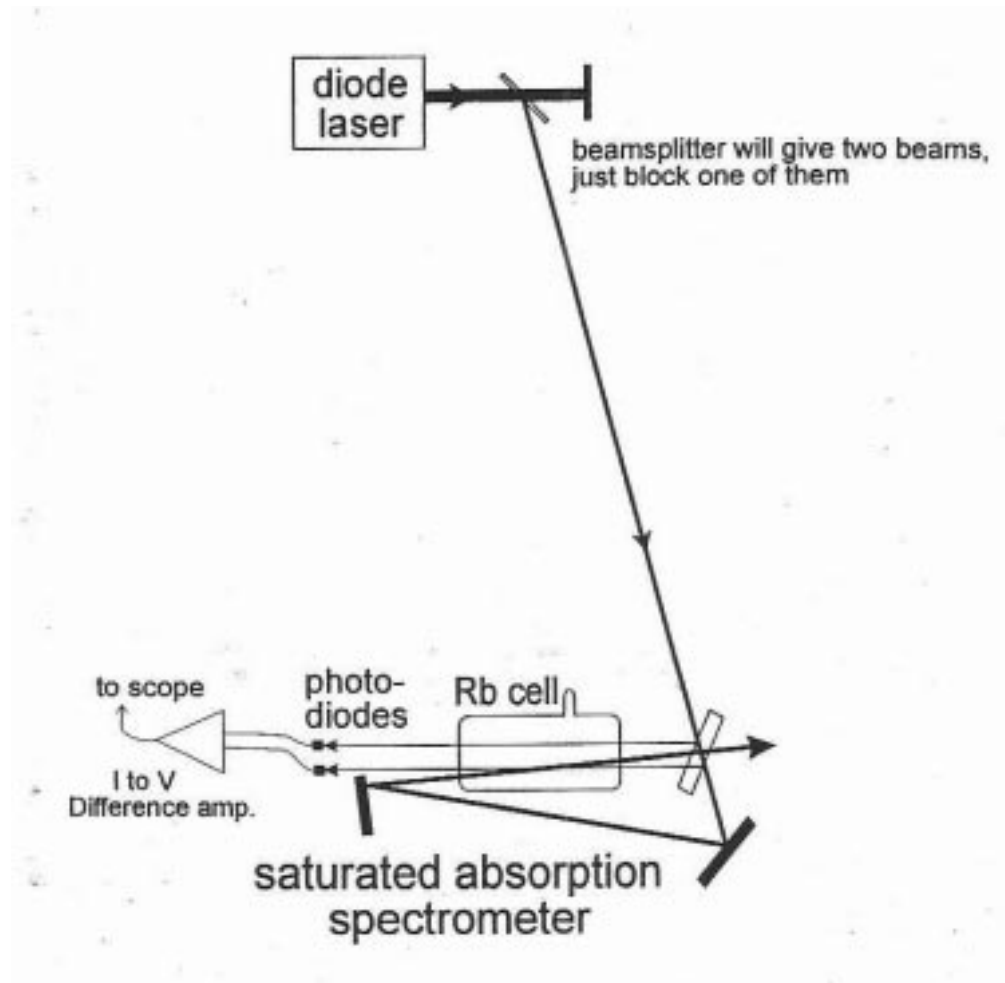


Figure 11. Apparatus for Doppler-free saturated absorption spectroscopy of ^{87}Rb .

If the second probe beam only is blocked then the signal from the first probe beam will be a nonlinear, saturated absorption spectroscopy signal “riding on” the Dopplerbroadened line. This signal is shown in figure 12b, where the two Doppler-broadened lines are the same transitions as in 12a, but note the hyperfine structure riding on these lines.

If the two signals in 12a and 12b are subtracted from each other, then the Dopplerbroadened line cancels and the hyperfine structure remains. The two photodiodes shown in figure 11 are wired such that their signals subtract, and the signal obtained when none of the beams are blocked is shown in figure 12c for ^{87}Rb . In 12c note that the amplitude of the triangular waveform is one-fourth as large as in 12a and b, that is, in 12c the laser is being swept over a range that is one-fourth as large as in 12a and b. The signal shown in 12c is the Doppler-free saturated absorption signal. We now consider in detail the physics behind figure 12.

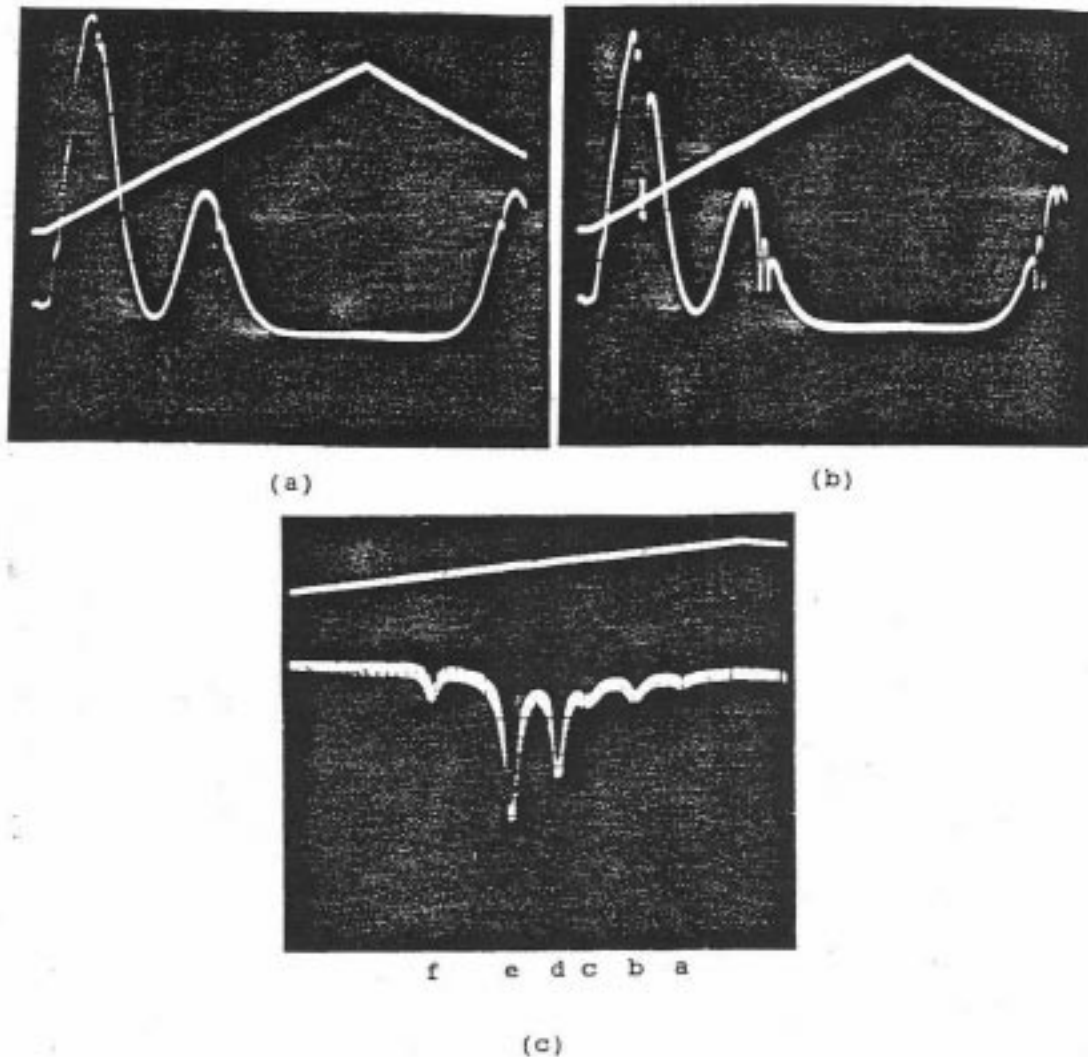


Figure 12. In all three photographs the frequency is increasing to the left. (a) Doppler-broadened spectral lines. (b) Doppler-broadened spectral lines with hyperfine structure. (c) Doppler-free saturated absorption spectral lines, where the spectral lines are labeled consistent with figure 9.

We start by focussing on the first probe and pump beams. The pump beam changes the populations of the atomic states and the probe detects these changes. Let us first consider how the pump beam changes the populations, and then we will discuss how these changes effect the first probe signal. As discussed above, because of the Doppler shift only atoms with a particular velocity v_z will be in resonance with the pump beam, and thereby be excited. This velocity dependent excitation process changes the populations in two ways, one way is known as “hyperfine pumping” and the other as “saturation”. Hyperfine pumping is the larger of the two effects, and it will be discussed first.

Hyperfine pumping is optical pumping of the atoms between the hyperfine levels of the $5^2S_{1/2}$ state. This happens in the following manner. Suppose the laser frequency is such that an atom in the $F = 1$ ground state is excited to the $F' = 1$ excited state. The $\Delta F = 0$ selection rule indicates that this state can then decay back to either the $F = 1$ or $F = 2$ ground states, with roughly equal probabilities. When it decays back to the $F = 1$ state it will be reexcited by the laser light and the process repeated. Thus after a very short time interval most of the atoms will be in the $F = 2$ state, and only a small fraction will remain in the $F = 1$ state. If the atoms never left the pump laser beam, even a very weak laser would quickly pump all the atoms into the $F = 2$ state. However, the laser beam diameter is small and the atoms are moving rapidly so that in a few microseconds the optically pumped atoms leave the beam and are replaced by unpumped atoms whose populations are equally distributed between the $F = 1$ and $F = 2$ levels. (You are ask to show below, in Exercise 12, that the populations of these two levels are essentially equal at room temperature with the laser turned off.) The average populations are determined by the balance between the rate at which the atoms are being excited and hence optically pumped, and the rate they are leaving the beam to be replaced by fresh ones. Without solving the problem in detail, one can see that if the laser intensity is sufficient to excite an atom in something like 1 microsecond it will cause a significant change in the populations of the $F = 1$ and $F = 2$ levels, that is, more atoms will be in the $F = 2$ level than the $F = 1$ level. This mechanism is called hyperfine pumping since the net effect is pumping electrons from the $F = 1$ ground hyperfine level to the $F = 2$ excited hyperfine level of the $5^2S_{1/2}$ state. Although the example used was for the $F = 1$ to $F' = 1$ transition, similar hyperfine pumping will occur for any excitation where the excited state can decay back into a ground state which is different from the initial ground state.

Exercise 12

With the laser off, the ratio of the number of atoms in the energy level $E_{1/2,2}$ ($J = 1/2, F = 2$), $N(E_{1/2,2})$, to the number of atoms in the energy level $E_{1/2,1}$ ($J = 1/2, F = 1$), $N(E_{1/2,1})$, is determined by Maxwell-Boltzmann statistics:

$$\frac{N(E_{1/2,2})}{N(E_{1/2,1})} = \exp\left(-\frac{E_{1/2,2} - E_{1/2,1}}{kT}\right) \quad (20)$$

Assuming a temperature of 295 K, show that the above population ratio is 0.999, hence the two levels are essentially equally populated with the laser off. You may want to refer to Exercise 4 and the discussion that precedes it in the Introduction to Magnetic Resonance.

Exercise 13

Show that laser excitations from $F = 1$ to $F' = 2$, $F = 2$ to $F' = 1$, and $F = 2$ to $F' = 2$ will also produce hyperfine pumping of the $5^2S_{1/2}$ ground state, where the first excitation produces a larger population in the $F = 2$ than in the $F = 1$ level, and the other two excitations produce the larger population in the $F = 1$ level. Also show that laser excitations from $F = 2$ to $F' = 3$ and $F = 1$ to $F' = 0$ will not produce hyperfine pumping of the $5^2S_{1/2}$ state. One way to show the production, or nonproduction, of hyperfine pumping for each case is to show the upward transition and all of the allowed downward transitions on an energy level diagram like that in figure 8c, where the hyperfine levels of the $5^2P_{1/2}$ state do not need to be shown since we are not interested in transitions to these levels.

The other process by which the laser excitation to an excited F' level changes the ground state population is known as saturation. It was pointed out in Exercise 10 that when an atom is excited to an F' level it spends 28 ns in this level before it decays back to the ground state. If the pump beam intensity is low, it will stay in the ground state for much more than 28 ns before it is reexcited, and thus on the average almost all the atoms are in the ground state. However, if the pump intensity is high enough, it can reexcite the atom very rapidly. One might expect that if it was very high it would excite the atom in less than 28 ns. In this case most of the population would be in the excited state and very little would be left in the ground state. In fact, because the pump laser can “excite” atoms down just as well as up, this does not happen. (You may want to refer to Exercise 6 and the discussion that precedes it in the Introduction to Magnetic Resonance.) For very high intensity a limit is reached where half the population is in the excited state and half is in the ground state. For realistic intensities the population of the excited state will be less than 0.5, something like 2 to 20 % is more typical. The effect of using high power to rapidly pump the atoms to an excited state is known as “saturating the transition” or just saturation. (In many references hyperfine pumping is also referred to as saturation.)

This saturation effect will be present on the transitions which have hyperfine pumping as well as the transitions which do not. However, it is generally a smaller effect than the hyperfine pumping. This can be understood by considering the intensity dependence of these two effects on the population. We previously indicated that the hyperfine pumping starts to become important when the excitation rate is about once per microsecond. From the discussion above, it can be seen that the saturation of the transition will become important when the excitation rate is comparable to the excited state lifetime, or once every 28 ns. Thus hyperfine pumping will occur at much lower intensities than saturation. The intensities you will be using are low enough that the hyperfine pumping will be substantially larger than saturation. This is also why the $F = 2$ to $F' = 3$ and $F = 1$ to $F' = 0$ signals are much smaller than the other transitions in the saturated absorption signals. As one increases the intensity these peaks will become larger relative to the other peaks for the same reason.

Summarizing, in the absence of laser light the $F = 2$ and $F = 1$ levels have nearly equal populations, and when the pump beam is on and tuned to either the $F = 1$ to $F' = 1$, $F = 1$ to $F' = 2$, $F = 2$ to $F' = 1$, or the $F = 2$ to $F' = 2$ transition, then hyperfine pumping produces a larger population in either the $F = 1$ or the $F = 2$ level.

We now ask, “How does the hyperfine pumping by the pump beam affect the first probe beam?” Well, in the arrangement of figure 11 imagine that all of the atoms in the Rb cell are at rest and consider what happens when the laser frequency ν_L is tuned to ν_0 , the frequency of an atomic absorption line of the Rb atoms, for example, the $F = 1$ to $F' = 1$ transition. The hyperfine

pumping by the more intense pump beam produces a smaller population in the $F = 1$ level than that in the $F = 2$ level. This means there are fewer atoms in the $F = 1$ level that will absorb power from the first probe beam, hence the number of photons in the first probe beam that reach the photodiode detector will increase. Now the second probe beam is interacting with a different group of atoms in the vapor cell, hence it is not influenced by the pump beam; therefore, the second probe beam's intensity at its photodiode detector will be less than that of the first probe beam. Thus after subtracting the two signals in the current-to-voltage converter, the resulting signal will show the difference between the two probe beams due to the effects of hyperfine pumping by the pump beam. Also both probe beams have the same Doppler broadened absorption (neglecting the effect of the pump beam), and the subtraction cancels this common absorption as shown in figure 12c, leaving only the pump beam induced difference.

The atoms in the vapor cell will, of course, not all be at rest; instead they will have a distribution of velocities given by equation 12, the Maxwell distribution. An atom that absorbs light at frequency ν_0 when at rest, will absorb laser light of frequency ν_L , where ν_L is given by equation 14, when the atom moves with velocity $\pm v_z$ along the axis of the vapor cell. Consider the Maxwell distribution of atomic velocities shown in figure 13, where the number of ground state atoms $N_{gs}(v_z)$ is plotted against the atom velocity v_z .

The positive z -axis is arbitrarily chosen in the direction of the probe beams. We will consider the three cases of figure 13 in order.

(a) $\nu_L < \nu_0$. Atoms moving toward the right are moving toward the pump beam and they will see its light blue-shifted. At appropriate positive v_z (equation 14), the light will be shifted to ν_0 in the rest frame of the atoms, where ν_0 is the frequency of a transition from an F level to an F' level. Atoms moving at this velocity v_z will absorb the pump laser light. The probe beam is moving to the right, hence atoms moving to the left with the same velocity magnitude will absorb the probe beams. It is important to recognize that the three beams are interacting with three different groups of atoms. The two probe beams are interacting with atoms in different regions of the vapor cell moving to the left with velocity v_z , while the pump beam is interacting with atoms moving to the right with velocity v_z . Also the more intense pump beam causes a greater reduction in the number of atoms in the ground state than the less intense probe beams as is shown in figure 13a. Subtraction of the two probe beams gives a null signal.

(b) $\nu_L = \nu_0$. Atoms with speed $v_z = 0$ in the region of overlapping first probe and pump beams can absorb light from both the first probe and pump beams. For the $F = 1$ to $F' = 1$ transition, for example, the pump beam depletes the population of the $F = 1$ level, and then the first probe beam passes through with reduced absorption. Reduced absorption of the second probe beam does not occur, hence subtraction of the two signals gives an absorption signal without Doppler broadening. The interaction is nonlinear in that the first probe signal depends upon the fields of both the first probe and pump beams.

(c) $\nu_L > \nu_0$. This is like (a) with directions reversed, and subtraction of the two probe beam signals gives a null result.

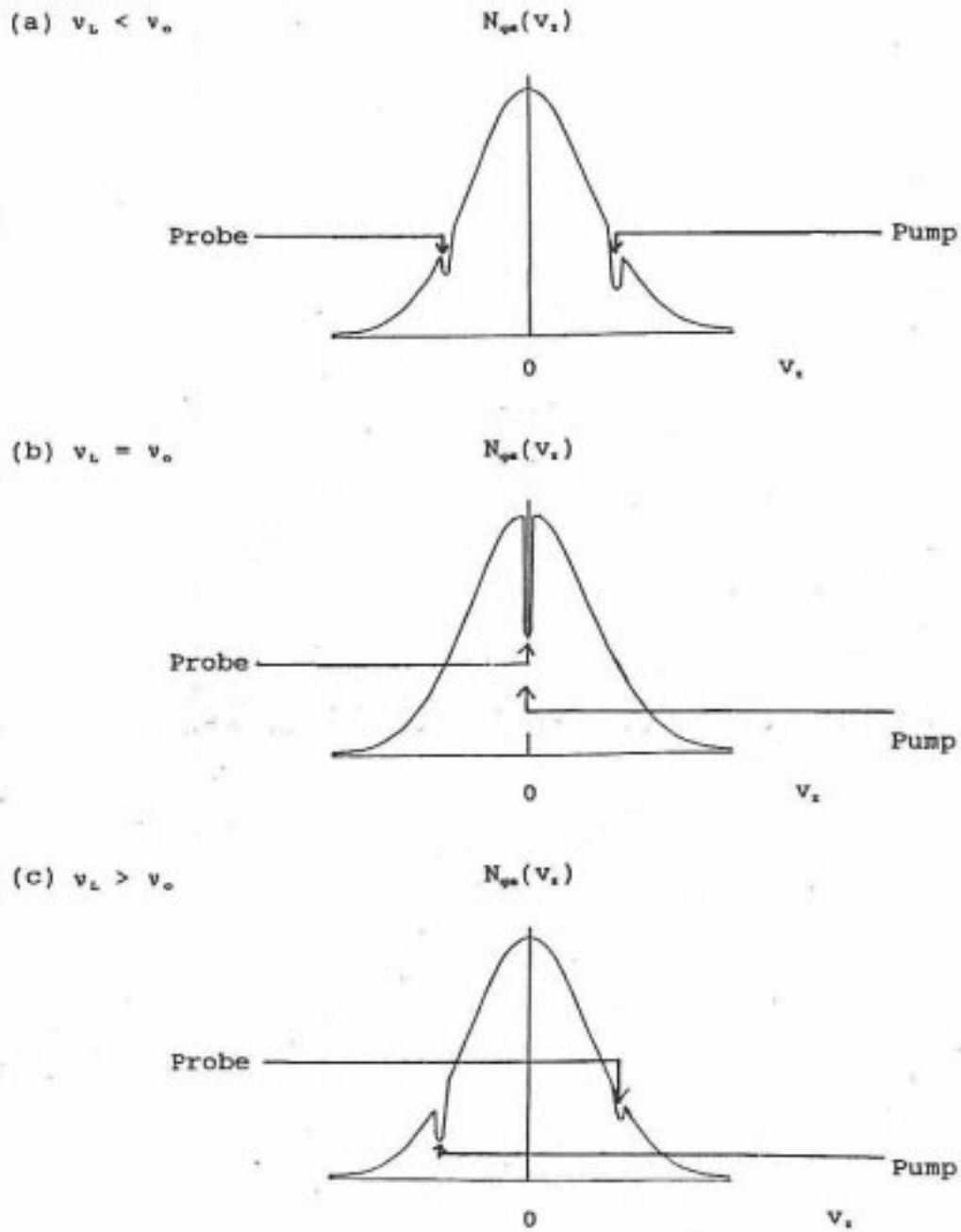


Figure 13. Absorption of pump and probe beams by ground state atoms, assuming a Maxwell velocity distribution, for the cases when the laser frequency ν_L is (a) $\nu_L < \nu_0$, (b) $\nu_L = \nu_0$, and (c) $\nu_L > \nu_0$.

A crossover peak appears midway between any two transitions that have the same lower level and two different excited levels. This occurs because, when the laser is tuned to the frequency midway between two such transitions, atoms with a particular nonzero velocity can simultaneously be in resonance with both the saturating beam and the probe beam and thus have nonlinear absorption. This happens because the two beams excite resonances to different transitions. For example, those atoms which are moving toward the probe beam with a velocity which gives a Doppler shift exactly equal to half the frequency difference between the two transitions will be shifted into resonance with the higher frequency transition. These atoms will see the pump beam with exactly the opposite Doppler shift. This shift will make the pump beam frequency just right to excite these same atoms to the lower frequency transition. As a result, the absorption is saturated not in stationary atoms but rather in two classes of moving ones.

Experiments

Remark: The diode laser used in this experiment is a research-quality instrument, and it should be handled with considerable care. It can be destroyed by a spurious voltage spike, for example, by a voltage induced in the current controller from other equipment. It is recommended that other equipment being used in this experiment be turned on and allowed to stabilize before the laser is turned on. Before discussing how to use the laser we consider the diode laser assembly shown in figure 14, which is reproduced from reference 1.

The labeled parts in figure 14 are: T-thermistor, LD-laser diode mount, C-collimating lens mount, G-diffraction grating, S-precision screw, P-PZT disk, MM-mirror mount, B-baseplate, H-controls horizontal motion of the grating, V-controls vertical motion of the grating, W-window. Lift the top off of the laser assembly and observe the parts. Also reference marks on the H and V knobs are desirable, for example, a white dot made with typewriter correction fluid on the top of each knob.

The discussion below assumes that the temperatures of the laser and the baseplate, the operating current, the position of the screw S, and the positions of the adjustments H and V have been made as described in reference I such that the laser wavelength is approximately 780 nm. The operating current and the knob settings for the temperature controllers should be recorded on or near the laser housing. Also the maximum laser current should be recorded.

The following adjustments **SHOULD NOT BE ALTERED:**

- 1 The precision screw S.
2. The vertical motion control V.
- 3 Baseplate or laser diode temperature.

The following should only be adjusted as specified later in the experiment:

4. Diode current.
5. The horizontal motion control H.

Turn off the laser in the following way, where the knobs and switches are on the current controller:

1. Set the laser current to zero using the current control knob.
- 2 Set the “run-short” switch in the short position.
3. Leave the power switch of the current controller in the on position.

To turn on the laser go through the three steps in reverse order, where the laser current should be set at the previously established value. **NEVER EXCEED THE MAXIMUM CURRENT.** Place an IR detection card in the beam path as you increase the laser current in order to observe the beam.

Diode Laser Power Output vs. Forward Current

The purpose of this measurement is to better understand the diode laser by measuring uncalibrated power output vs forward current. Wire the current to voltage amplifier circuit shown in figure 15 or use a box which contains this circuit already wired. The OP913 SL is a PIN silicon photodiode with a large active area chip. Other photodiodes may be used in its place if available. Place the OP913 between M1 and M2 shown in figure 11 such that it intercepts the pump beam. Measure the output voltage from the amplifier as a function of the diode laser forward current, but do not exceed the specified operating current. Plot your data, where the resulting curve should resemble those shown in figure 5. After finishing these measurements set the current at the operating current.

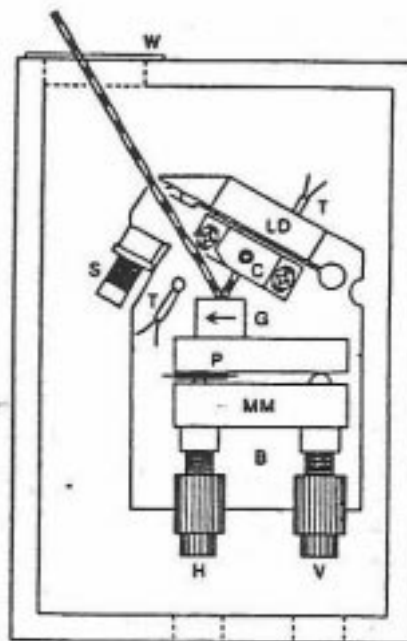


Figure 14. Assembly top view of laser.

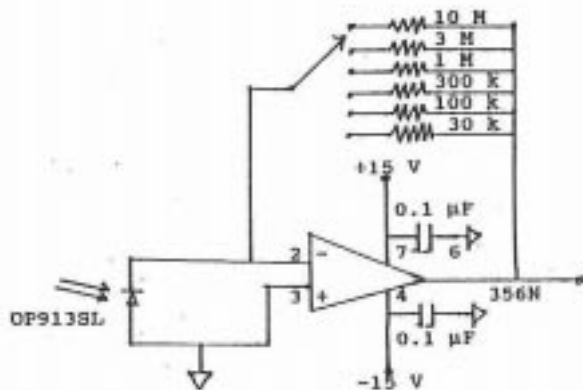


Figure 15. Circuit to measure uncalibrated diode laser power output as a function of diode laser current. The switch should be a shorting switch.

Remark: If the laser light saturates the photodiode, then you can reduce the laser intensity by inserting pieces of darkened plexiglass in the beam. By using several pieces, you can measure the transmission of a single piece.

Exercise 12

What is the threshold current for your laser?

Remove the OP 913 photodiode from the path of the pump beam.

Doppler-Broadened Spectral Line

In this part of the experiment you will observe the Doppler-broadened line without hyperfine structure riding on it, that is, you will observe a signal similar to that shown in figures 12a.

The first step is to tune the laser frequency to either the $F = 1$ to F' transition or the $F = 2$ to F' transition. Methods of tuning and typical tuning rates are: (1) diode laser current: 200 MHz/mA, (2) piezoelectric tuning: 1 GHz/V, (3) grating change by horizontal motion control H: 5×10^3 GHz/turn, (4) temperature-change of the laser: 4 GHz/°C. When the laser is tuned to either transition the vapor cell will fluoresce along each beam path. The fluorescence may be observed with either a hand held IR viewer or a CCD surveillance camera. If neither device is available, then place the IR detection card near the cell such that you can observe IR radiation reflected from the card.

To search for fluorescence:

1. Start with the laser and baseplate temperatures and the knob H set at the established values.
2. Turn on the triangle wave generator with the gain set at the maximum value.
3. Look for fluorescence as you tune the laser current by about ± 10 mA about the established value, but do not exceed the maximum value. If you do not see the fluorescence, then set the current at the established value, rotate H about $\pm 1/8$ of a turn about the established value, and at each extreme value of H vary the current by ± 10 mA. If fluorescence is not observed, then see your instructor.

She/he will probably first check the vertical alignment by seeing if the vertical tilt is set to give the lowest threshold current. If the vertical alignment is correct they will probably adjust the laser temperature, but not the baseplate temperature, in 1 °C steps repeating step 3 at each temperature.

Once fluorescence is observed block the second probe beam such that it does not reach the photodiode shown in figure 11. (It does not matter if the beam is blocked before or after passing through the vapor cell.) Block the pump beam before it reaches the vapor cell, for example, between M1 and M2 in figure 11. Trigger the scope from the sync out pulse of the triangle wave generator. Adjust the offset of the triangle wave generator and, if necessary, make slight adjustments in the laser current until the spectral line of ^{87}Rb is centered on the triangle waveform as shown in figure 1 2a. Record the signal with the data acquisition system at your station, for example, a scope camera.

Doppler-Broadened Line with Hyperfine Structure

Remove the block from the pump beam. You should observed a Doppler-broadened line with hyperfine structure riding on it, somewhat like that shown in figure 12b. Record the observed signal. BE SURE AND RECORD THE PZT VOLTAGE SCALE FOR ALL SPECTRA. YOU WILL LATER USE THE MICHELSON TO CONVERT THIS VOLTAGE INTO FREQUENCY.

Doppler-Free Saturated Absorption Spectral Lines

Remove the block from the second probe beam, and, hence, observe Doppler-free saturated absorption spectral lines. Reduce the gain of the triangle waveform generator and observe the effect on spectral line resolution. Insert tinted plexiglas or microscope slides

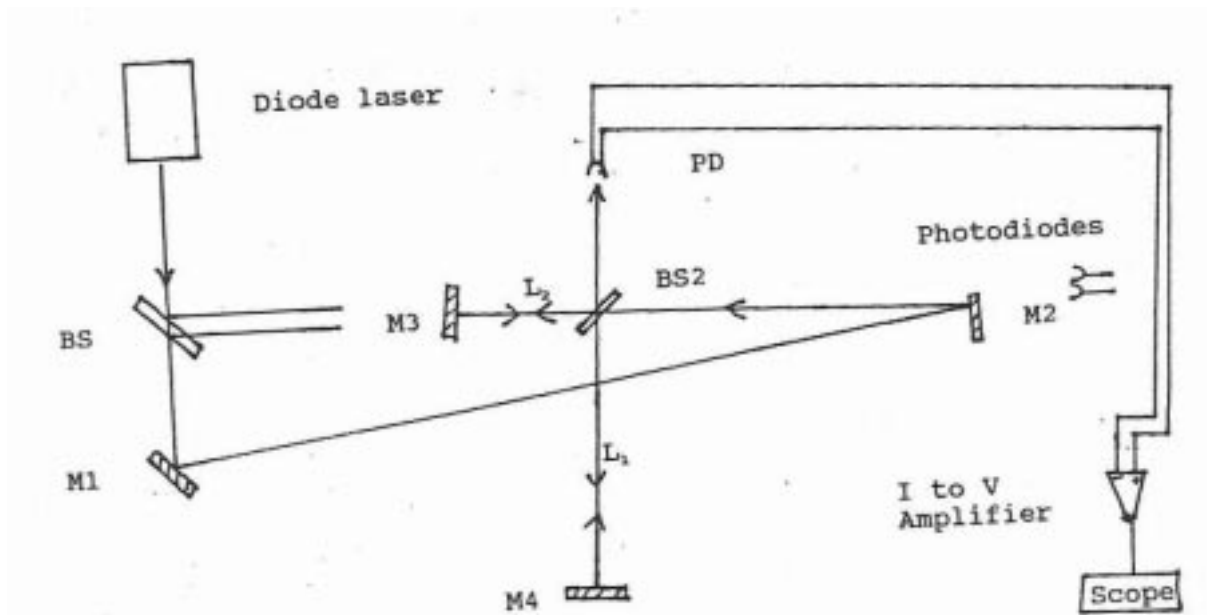


Figure 16. Michelson interferometer.

between the laser and the beam splitter, hence observe the signal using reduced laser power. Record the signal.

Now tune the laser, as described above, to the other transitions so that you observe transitions from both hyperfine ground states of ^{87}Rb ($F=2$ to F , and $F=1$ to F'), and from both ground states of ^{85}Rb ($F=2$ to F' , and $F=3$ to F) and record similar data. Figure 12c shows the $F = 2$ to F' transitions for ^{87}Rb .

Calibration: Michelson Interferometer

A Michelson interferometer will be used to calibrate the horizontal axis of the oscilloscope in frequency units. Without altering the laser adjustments, remove the vapor cell shown in figure 11 and mount the mirrors M3 and M4, the beam splitter BS2, and the photodiode PD as shown in figure 16, where for convenience the current controller, temperature controller, and triangle wave generator are not shown. Disconnect the photodiodes from the I to V amplifier and connect PD to the amplifier.

The beam is split by BS2 (a microscope slide is an adequate beam splitter), and the two beams are recombined at BS2 after they have traveled distances of $2L_1$, and $2L_2$. After returning to BS2, and thereafter, the two beams will have a phase difference due to their path difference given by:

$$\begin{aligned} \phi_1 - \phi_2 &= \frac{(2L_1 - 2L_2)}{\lambda} 2\pi \\ &= \frac{2\nu}{C} (L_1 - L_2) 2\pi \end{aligned} \quad (\text{rad}) \quad (21)$$

where ν and c are the wave frequency and velocity. The frequency is not fixed, rather it is being swept by the triangle waveform applied to the PZT, hence as the frequency changes the phase difference will change. The changes in frequency and phase are expressed by writing equation 21 as

$$\Delta(\phi_1 - \phi_2) = 2 \frac{\Delta\nu}{c} (L_1 - L_2) 2\pi \quad (22)$$

The intensity of the two superimposed waves, aside from a constant of proportionality, is given by,

$$\begin{aligned} I &= E \bullet E^* = (E_1 e^{i(\frac{2L_1}{\lambda} 2\pi - 2\pi\nu t)} + E_2 e^{i(\frac{2L_2}{\lambda} 2\pi - 2\pi\nu t)}) \\ &\bullet (E_1 e^{i(\frac{2L_1}{\lambda} 2\pi - 2\pi\nu t)} + E_2 e^{i(\frac{2L_2}{\lambda} 2\pi - 2\pi\nu t)}) \quad (23) \\ &= |E_1|^2 + |E_2|^2 + 2E_1 \bullet E_2 \cos \Delta(\phi_1 - \phi_2) \end{aligned}$$

where \bullet was inserted to indicate the change in the phase from sweeping the frequency. The interference is a maximum whenever

$$\Delta(\phi_1 - \phi_2) = 2\pi \quad (24)$$

Substituting equation 24 into 22 yields the frequency spacing of the interference maxima

$$\Delta\nu = \frac{c}{2(L_1 - L_2)} \text{ (Hz)} \quad (25)$$

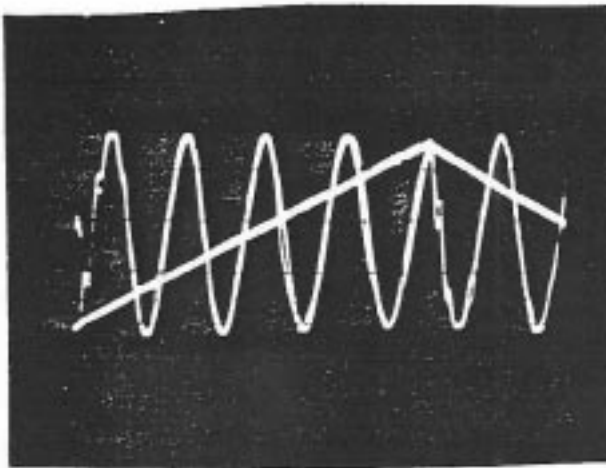


Figure 17. Interference fringes and the triangle wave sweep. In this case: $L_1 - L_2 = 19.5$ cm, and $\bullet\nu = 0.769$ GHz.

Figure 17 is a photo of the scope screen showing the triangle waveform and the interference pattern, where the frequency spacing between maxima is given by equation 25.

There are a few things it is helpful to know in order to get good fringes from the interferometer. First, you should not be misled by the weak fringes you will get from the interference of the beams reflecting off the two sides of the beamsplitter.

They will not have the correct spacing and they will not require both beams returning off M3 and M4. Second, you need to realize that in order to give good fringes the two beams must not only overlap at the photodiode, but they must also be parallel. It is possible to have them come back from M3 and M4 and go through different parts of the beamsplitter but still overlap at the photodiode. By drawing some simple triangles you should be able to convince yourself that in this case the path length difference $L_1 - L_2$ will be different at different places where the beams overlap. This will result in a series of bright and dark fringes across the photodiode which you can see if you look closely with the viewer. If the phase difference across the face of the photodiode is a full 2π there will always be a bright and dark fringe present and changing the laser frequency will give no change in the total power on the photodiode, and hence no signal. The larger the angle between the beams the closer will be the spacing of the fringes. As you adjust the beams to be parallel (but still overlapping) the spacing between the dark fringes will become larger until it is as large as the photodiode, and you will see a large modulation in the photodiode output as you change the frequency. Often the easiest way to get good fringes is to first make the beams as parallel and overlapping as possible and then do the final adjustments by looking at the photodiode output and align the beams to get the largest fringes as you ramp the laser frequency. The final thing you need to realize is that you want the beams to go nearly but not exactly back along the incident laser beam. If they are going exactly back they will go back into the laser and cause the frequency to jump around. This usually shows up as a lot of noise on the fringe pattern signal you see on the oscilloscope. If you keep these things in mind you should not have trouble aligning and using the Michelson interferometer with the following procedure.

Choose L_1 and L_2 such that ν is approximately 0.5 GHz, and start with the amplifier gain set to 100 k \times .

1. Place an IR detection card over PD and adjust the tilts of M3 and M4 such that the two beams are superimposed.
2. Place the IR detection card on M1 near the beam spot incident from the laser, adjust M3 and M4 such that the two spots coming from BS2 are superimposed on each other but slightly offset from the beam spot incident from the laser. Check the superposition of the two spots at PD, re-align if necessary. Once alignment is achieved the scope trace should resemble figure 17.

Carefully calibrate the horizontal axis of the oscilloscope for the gain setting of the triangle wave generator you used in measuring the spectra. If you determine how large a frequency change is produced for each volt that is applied to the PZT drive, you can then convert the horizontal scale of the spectra from ramp voltage to frequency, and then determine splittings and linewidths. You might check that different ranges on the ramp generator give the same calibration factor.

As the laser frequency is changed you will observe a cosine modulation on the oscilloscope. However, if you make a large sweep you will see sudden jumps in the signal as if the phase has abruptly changed. What has actually happened is that the laser has jumped to a different frequency (a so called "modehop"), probably one which corresponds to one more or one less half wavelength fitting into the laser cavity as defined by the diffraction grating "mirror" and the high reflecting facet of the diode chip, and hence is different by about 3 GHz. The frequency where the laser jumps will move if you change the laser current. It could also be jumping to a frequency which corresponds to one more or one less half wavelength fitting into the actual diode chip itself. This causes a much larger change in the frequency. Under ideal conditions with this laser setup you can get a scan of about 8 GHz without a modehop. A single scan of this

length, which shows all 4 rubidium peaks at once, is shown in fig. 18. More typically you will get continuous scans (no mode hops) of 3 or 4 GHz. If the frequency range over which you get a continuous scan is shorter than this it probably means that the vertical alignment is off. The length of continuous scan can also be affected by the laser temperature.

Data Analysis

1. Measure the FWHM for each of the two Doppler-broadened lines of ^{87}Rb . Compare your values with your calculated value from Exercise 9.

2. Measure the separation of the hyperfine lines for the $F = 2$ to F' transitions, use equation 13 to obtain a theoretical expression for the frequency separation of the hyperfine lines, and then solve for the constants A and B for the $5^2\text{P}_{3/2}$ state of ^{87}Rb . Compare your results with the accepted values given earlier. If you have time, carry out the same analysis for the other transitions.

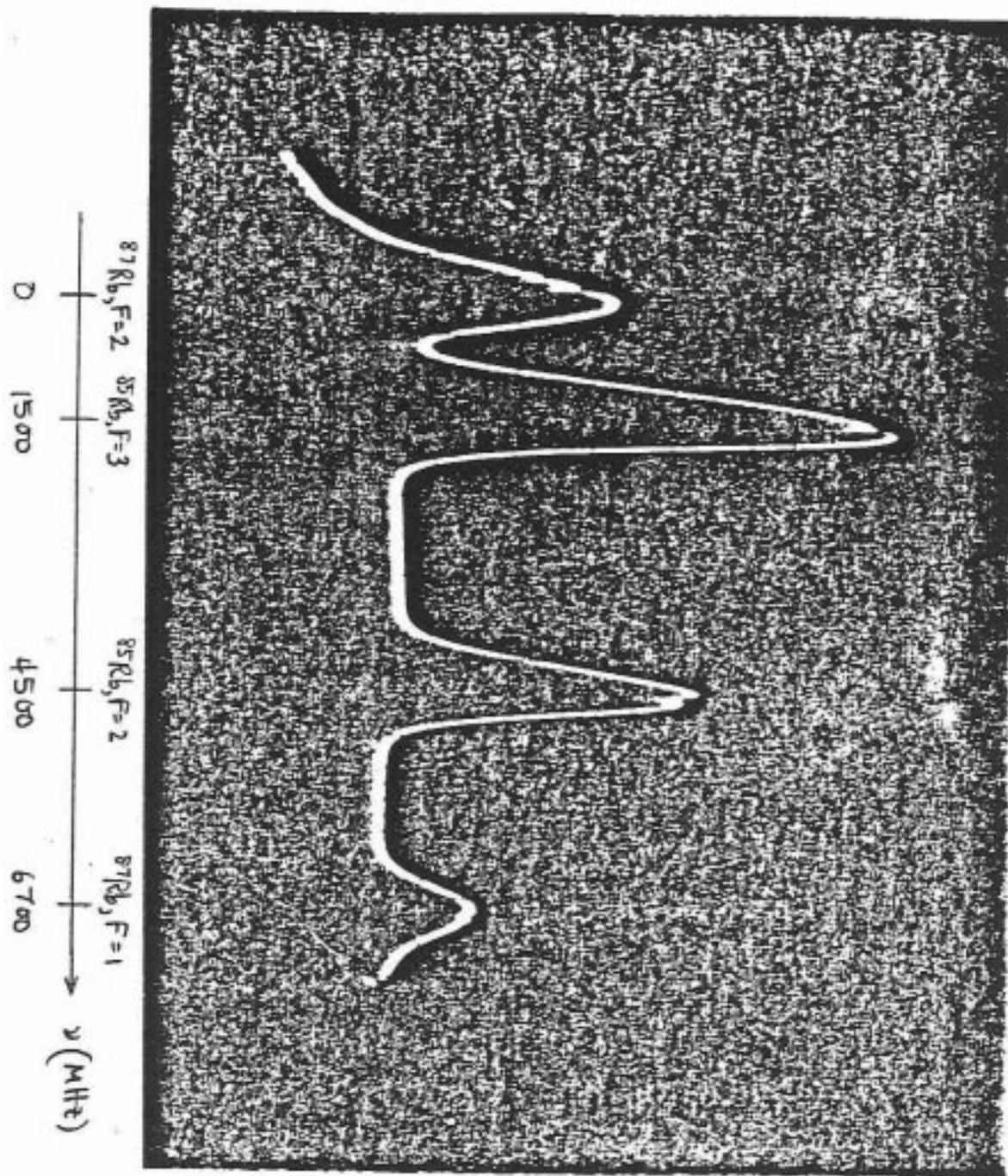


Figure 18. Absorption spectrum for the two rubidium isotopes